139

MEASUREMENTS OF WIND LOADS ON FULL-SCALE GLASSHOUSES

D.A. WELLS and R.P. HOXEY

National Institute of Agricultural Engineering, Silsoe, Bedfordshire MK45 4HS (Gt. Britain)

Summary

   Reliable prediction of the wind loads on the structure and cladding of glasshouses is essential to their safe and economic design. To provide data on wind loads, measurements were made on five shapes of glasshouse, under natural wind conditions and generally over a 90° range of direction.
   The experimental procedure is described and detailed results are presented together with an outline of the data analysis by a novel technique which takes into account short-term fluctuations in wind direction.
   Consideration is given to the parameters which must be included in a rationalised design procedure and a simplification of the detailed results is presented in the Appendix in a form which would be convenient for use in design and which is readily comparable with established codes.

1. Introduction

   In Europe and North America, over 20000 ha of glasshouses are in use for the production of flowers and vegetables. As with other buildings, their efficient structural design can only be achieved if the loads to be sustained can be estimated adequately. The least well defined of the major loads on glasshouses are those due to wind pressure and, despite a construction rate in the U.K. of approximately 120 ha per annum over the past decade [1], virtually no reliable design data on wind loads are available to the designer.
   Because of the random nature of the occurrence and intensity of strong winds, some difficulty in estimation of design speeds is inevitable. Nevertheless, analysis [2] of the distribution of extreme values recorded over 10 years or more allows the prediction of design speeds on a probability basis. However, while the aerodynamic aspects of a building's response to known winds are amenable to experimental determination, they are at present only poorly defined for many buildings.
   Although the major part of the U.K. glasshouse area of 1600 ha consists of multi-span structures, only very scant data of dubious validity are available for buildings of this type. In the U.K., wind load design data are set out in British Standards Code of Practice No. 3 [3] (CP3) and for multi-span buildings under transverse winds the code gives data (based on 'fragmentary evi-

dence') for roof angles of 20° and 30°; the slope of 26° normally used for glasshouses is not covered and lies in a region of rapidly changing load.

Because of the difficulties of making measurements in the natural wind, many of the data in CP3 (and indeed in most other national codes) have been obtained from model tests under uniform smooth flow conditions in wind tunnels. There are now serious doubts [4—6] as to the validity of the application of these results to real structures exposed to the turbulent shear flow of atmospheric winds.

It is against this background that a programme of measurements on full-scale glasshouses was undertaken.

2. Apparatus and experimental procedure

2.1 Houses and sites

Measurements were made of external and internal pressures on five houses (Table 1) and of internal pressures on a further five houses. These were chosen to be characteristic of the existing glasshouse stock, yet at the same time to take into account emerging trends in design. A comparison of the transverse sectional geometries of the buildings on which external pressures were measured is shown in Fig.1.

Houses 04 and 05 were instrumented for limited measurements under transverse wind conditions only. Houses 01, 02 and 03 were in the Southport/Preston area, the others being in the Bedford and Hertford area, and this combination of locations was found to provide excellent opportunities for frequent and convenient data collection.

All the houses were in open country, well exposed to prevailing winds. It is under such conditions that design wind speeds are likely to be maximal, and it is thus appropriate that coefficients for use in the design of mass-produced buildings should be derived under corresponding conditions of wind velocity profile ($\alpha = 0.15$ to 0.22, see section 2.2.1).

TABLE 1

Details of experimental glasshouses

House ref.	No. of spans	Span width (m)	Overall width (m)	Length (m)	Eaves height (m)	Ridge height (m)	Roof angle (deg)	Eaves height/span width ratio
01	1	6.4	6.4	21.3	2.4	3.9	26	0.37
02	7	3.2	22.4	63.0	2.4	3.1	26	0.73
03	6	6.6	39.7	79.6	2.4	4.0	26	0.36
04	2	12.8*	25.6	39.6	3.4	7.1	26	0.26
05	8	6.4	51.2	88.8	2.8	3.9	20	0.44

*Asymmetric spans.

01
1 x 6.4 m span
26° roof angle

02
7 x 3.2 m spans, 26° roof angle

03
6 x 6.6 m spans, 26° roof angle

04
2 x 12.8 m spans, 26° roof angle
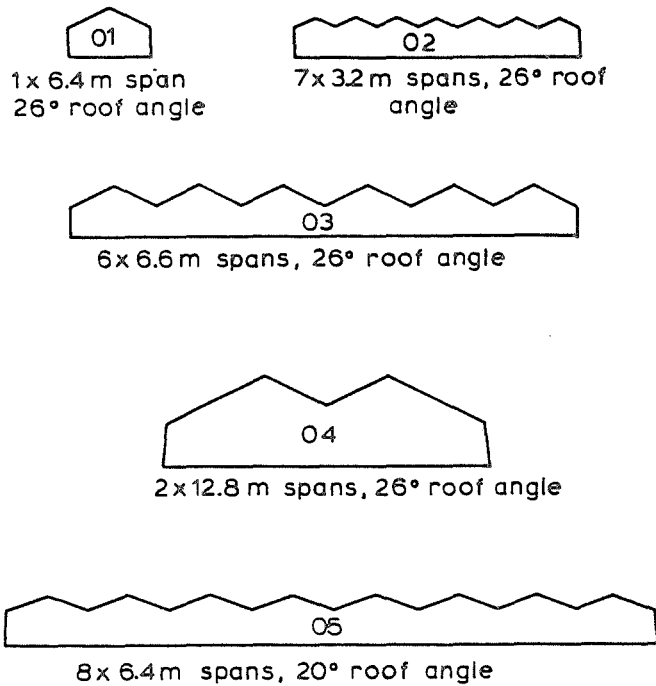
05
8 x 6.4 m spans, 20° roof angle

Fig. 1. Transverse sections of glasshouses.

2.2 Instrumentation

The determination of a pressure coefficient (C_p) characterising wind loads requires the measurement of the load at a point on the glasshouse surface and of the causative wind to which the load must be related. Apparatus [7,8] of appropriate response was developed to record free stream wind pressure and direction, together with the resulting pressures at 48 points (24 in the case of house 04) distributed over the surface of each glasshouse. The overall frequency response of both the wind pressure and the wind load measuring systems was 0—2.5 Hz (3 dB down) for wind speeds exceeding 8.5 m s^{-1}.

The load-bearing structure of glasshouses consists of roof truss (or space frame) and stanchion assemblies spaced 3—6 m apart. These may be treated by the designer either as separate structural entities or as enjoying some degree of structural continuity with adjacent assemblies. A gust speed averaged over 5 s is given by CP3 as appropriate in the structural design of all buildings up to 50 m in horizontal or vertical extent. Gusts of such spatial extent will thus envelop large sections of glasshouse embracing many structural units. Maximum loads are thus likely to be developed on, and will require to be sustained by, individual structural units, since it is highly unlikely that a unit

could derive significant reinforcement from another some 50 m distant. Simultaneous measurement at all points is thus unnecessary and the load pattern can be determined progressively to give a valid measure of the maximum integrated load. Accordingly, signals from pairs of measuring points were recorded sequentially, only two pressure transducers being used to measure the loads at 48 points. The adoption of this approach allowed considerable simplification and economy in sensing and recording instrumentation.

2.2.1 Wind pressure and direction measurement

A pressure tube anemometer/windvane combination was used for wind measurement. This type of instrument has an inherently fast response to wind variation, the kinetic energy of the air being measured as a dynamic pressure at the end of a horizontal tube held into the wind by a vane. Transducers provided electrical analogues of wind pressure and vane position to a four-channel FM tape recorder.

For all measurements on houses 01, 02 and 04 and for the early ones on house 03, pressure tube anemometers of a modified Dines [9] type were permanently mounted at each site on 10 m masts. However, because of maintenance difficulties, all later measurements were made using a directional pitot tube of similar response characteristics. This was mounted at ridge height on a portable sectional mast erected on each recording occasion. A reference source against which the total pressure from the directional pitot tube could be measured was provided by a calibrated static pressure probe (to a design by the National Bureau of Standards, U.S.A.) mounted on the sectional mast.

The presentation of results based on wind pressure at ridge height is now considered appropriate for design, and the wind pressure data from the earlier measurements at 10 m were corrected to ridge height using relationships of the form $V_h/V_{10} = (h/10)^\alpha$ derived from wind pressure/height data appropriate to the site and time of year [10].

2.2.2 Wind load measurement

The commercial glasshouses selected for measurements had the usual requirement for high light transmission which could not have been maintained had opaque pressure plate transducers of the type used by other workers [11] been installed. Accordingly, a simple pressure tapping in transparent acrylic sheeting was devised which could be installed at any position on a glasshouse surface in place of glass panes. The pressure tapping consisted of a 9.5 mm hole at the centre of a stiffened acrylic sheet, a cemented acrylic boss retaining a tubular extension of the hole to give a tapping some ten diameters in length. The assembly terminated in a porous (2 μm) ceramic plug which drained off very effectively any rainwater entering the tapping point. The pressure signals were conveyed by flexible tubing and automatically switched in pairs to two transducers of the same type as those used for wind measurement and which provided signals to the remaining channels of the recorder.

For those measurements where the modified Dines anemometer was used (section 2.2.1), the calibrated reference [8] against which wind loads were measured was provided by a 0.05 m³ open tank sunk flush into open level ground remote from the glasshouse. For all subsequent measurements, the NBS static pressure probe was used as the reference source.

A preliminary study in a wind tunnel had indicated that the load measured at a central tapping point would be affected by the glazing bar upstand (~20 mm). Measurements were made under natural wind conditions on a full-scale glasshouse which established that the mode of load variation is wind-direction dependent and is such that the measured load is slightly higher (from 0 to 0.16 C_p depending on location) than the mean [12]. The measurements allowed correction terms to be obtained for all surfaces and these corrections have been applied to all data given in section 3.

2.3 Calibrations and zero corrections

Pressure transducers were calibrated periodically in the laboratory against a Betz micromanometer by applying static pressure loads. Additional checks were made on-site by applying a common dynamic pressure (from the anemometer) to all three transducers. The signals from these were recorded in the usual way and yielded calibrations which were used in the data analysis.

During analysis, corrections were also made for the effect of any instability of the transducers, amplifiers and tape recorder zeros, by taking into account zero pressure signals which were generated for a few seconds at the beginning and end of each pressure tapping record.

2.4 Data recording and analysis

Generally, data were recorded for 48 tapping points (47 external, 1 internal) over a 90° span of wind direction to determine the load distribution over the surface of each house. Recordings of 240 s duration were taken in sequence from pairs of tappings together with continuous wind pressure and direction data. Chart records were also taken during data collection so that an immediate visual check could be maintained.

Magnetic tapes of 240 s duration per tapping point were digitised at 6.5 data points per second onto eight-hole paper tape for subsequent analysis by computer.

For the experiments where anemometers mounted at 10 m were used, pressure coefficients have been based on comparisons of mean loads and pressures, time-averaged over 1.05 s and are considered to be operative at the mean wind direction. Data from the later experiments (where wind was measured at ridge height) have been similarly time-averaged but analysed by a method [13] which takes into account the considerable variations in wind direction (~40°) which can occur during a 240 s recording period.

Pressure coefficients are dependent on the direction of air flow and the considerable variation in flow direction prevents the derivation of a meaningful C_p from a direct comparison of the probability density functions (PDF) of wind load and wind pressure. Such a method results in a wide range in the value of C_p; a comparable spread of coefficients had been observed by other workers [14] to result from their similar comparisons of pressures on dwelling houses. To overcome this problem, C_p was assumed to be a single-valued function of wind direction and derived by comparison of the PDF of wind load and the PDF of $\{C_p \cdot q\}$ such that the difference between the PDFs was minimised with respect to C_p.

The method of solving the constraint equation was to assume a quadratic relationship between C_p and wind direction. The constants of the quadratic equation were optimised by an iterative method which minimises the sum of the weighted squares of the differences in the PDFs at the 0 (5) 100 percentile points. The weighting function was derived from an analysis of errors at the 0 (5) 100 percentile points due to sampling the wind vector remote from the building. The residual errors in the comparison of PDFs were found to be small and less than the standard error due to sampling.

This method of analysis has been carried out on many data sets and the assumption that C_p can be represented as a single-valued function of wind direction has been empirically justified [13]. The values of pressure coefficients so obtained are equivalent to the quasi-static mean values as employed in CP3, and this justifies the values as suitable for use in design. From analyses of power spectra of wind loads and wind pressures, there is no evidence that pressure coefficients derived in this way are significantly diminished by the loss of structure-generated turbulence and they are therefore applicable in regions where local coefficients are given in CP3.

The quadratic analysis has been found to be most efficient when the wind pressure and direction have been directly recorded at tapping point height rather than synthesised from observations at 10 m. Thus, for the earlier data, this technique was not used and coefficients, considered to be effective at the mean wind direction, were derived from mean loads and pressures. Good agreement was found between coefficients so obtained and those given by the quadratic equation for the same wind direction.

A considerable reduction in the amount of data necessary to define a loading pattern results from the application of the quadratic analysis, since a single 240 s recording yields, over a limited range, the mode of variation of pressure coefficient with wind direction.

2.5 Internal pressure measurement

Since glasshouses are permeable structures, with little standardisation of
door and ventilator positions, the measurement of internal pressure was made
on an extended range of houses. An additional five houses were chosen to augment
the houses on which external wind pressures were measured. All were exposed
structures selected to cover a range of commercial glasshouse manufacture
and glass retaining methods. Details of the glasshouses and a summary of the
results appear in section 3.2 of this report.

2.6 Frictional drag

The full-scale measurements made under natural wind to determine the
loading pattern created by the glazing bar upstand gave the pressure on each
side of the bar and hence the profile drag on the surface [12]. Although
measurements were only made on a single-span glasshouse, a theoretical model
was fitted to the results and frictional drag computed for the range of struc-
tures.

3. Results

3.1 External pressure coefficients (C_{pe})

For the five glasshouses on which external pressures were measured, the
results are presented in Tables 2 to 6 for a range of wind directions. Each table
is accompanied by a site plan and tapping point plan (Figs. 2—6). Pressure
coefficients are relative to wind pressure at ridge height and where this was
derived from wind pressure measured at 10 m a mean value of the exponent
for the velocity profile (α) is given. Corrections have been made for the effect
of the glazing bar upstand on the pressure sensed at the central tapping point,
and coefficients presented represent the mean pressure over the glass pane.

Although the buildings were selected for their excellent windward expo-
sure, there were, however, obstructions on the leeward side, and reference
should be made to Figs. 2—6 when comparing pressure coefficients to ensure
that account is taken of these obstructions.

3.2 Internal pressure coefficients (C_{pi})

Internal pressure coefficients for houses 01, 02, 03, 04 and 05 are presented
in Tables 2—6. In all cases, results are given for doors and ventilators in the
closed position but additionally in Table 3 for 02 with the ventilators 5—10%
open.

For the glasshouses on which internal pressure measurements only were
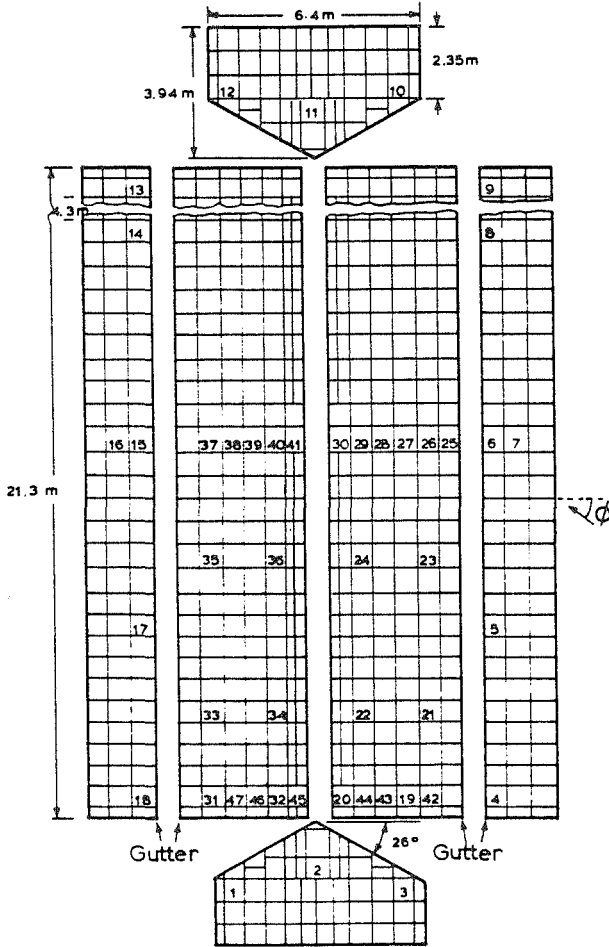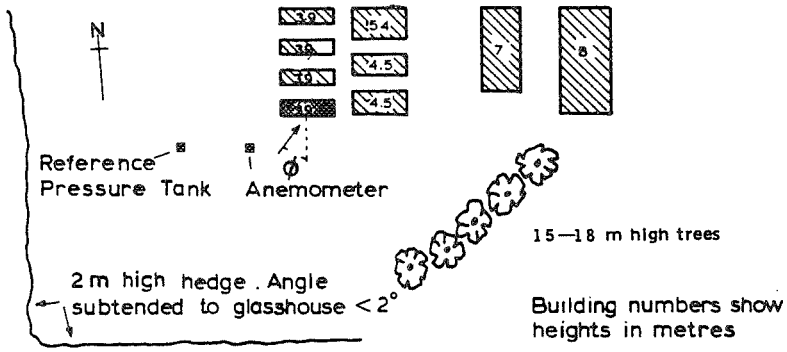made, results are given in Table 7 for transverse and longitudinal wind direc-

146

Fig.2. Site and tapping point plan for house 01.

TABLE 2

Pressure coefficients for house 01 — single 6.4 m span

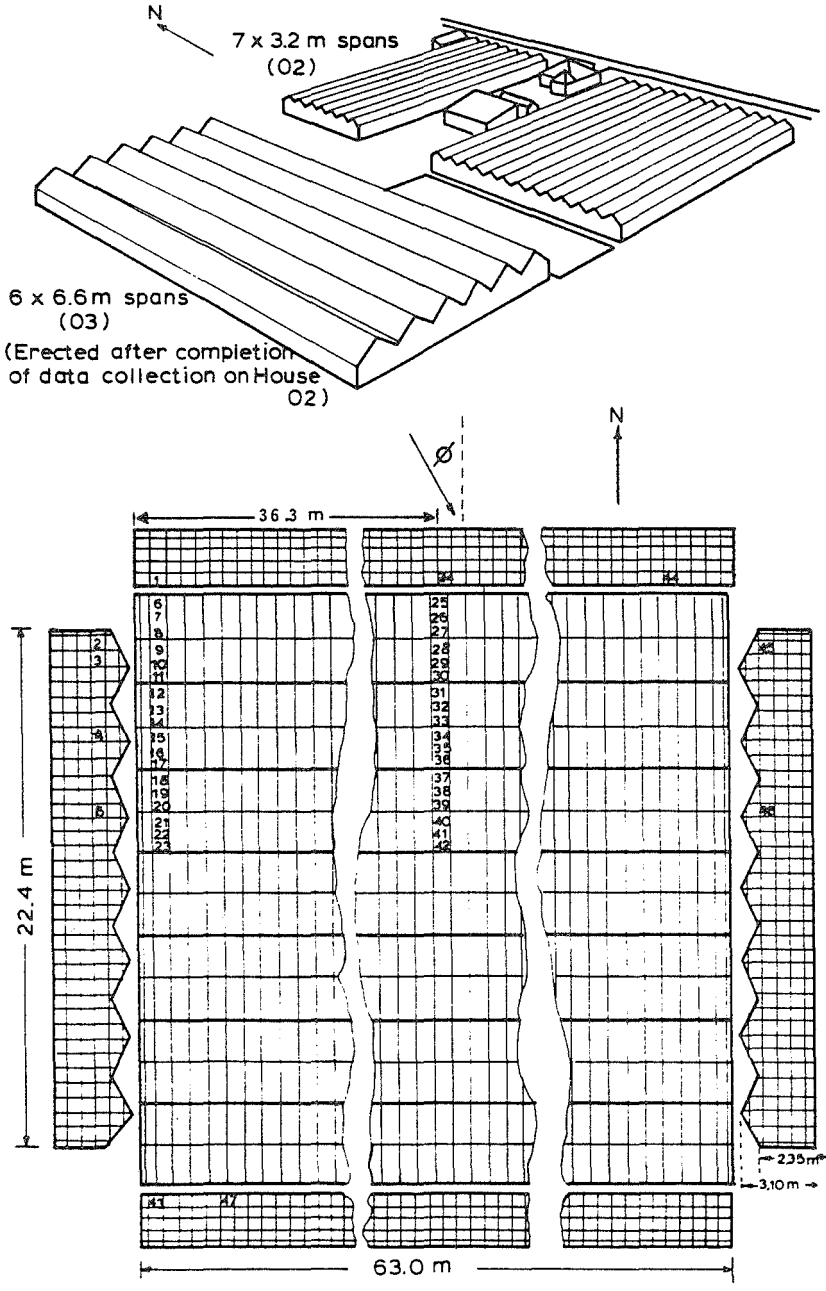| Tapping point		Coefficients relating loads to wind pressure at ridge height ($\alpha = 0.16$)				
No.	Height (m)	Wind angle ϕ (deg)				
		0	22.5	45	67.5	90
1	1.98	−0.46	−0.02	0.31	0.45	0.51
2	2.66	−0.62	0.11	0.57	0.79	0.85
3	1.98	−0.61	0.36	0.77	0.65	0.51
4	1.98	0.56	0.63	0.24	−0.56	−0.95
5	1.98	0.60	0.52	0.27	0.03	−0.13
6	1.98	0.51	0.43	0.26	0.08	−0.04
7	1.38	0.46	0.39	0.26	0.06	−0.06
8	1.98	0.60	0.49	0.27	0.08	−0.02
9	1.98	0.56	0.43	0.15	0.01	−0.01
10	1.98	−0.61	−0.41	−0.20	−0.06	0.01
11	2.66	−0.62	−0.34	−0.18	−0.09	−0.05
12	1.98	−0.46	−0.41	−0.16	−0.02	0.01
13	1.98	−0.95	−0.30	−0.07	−0.03	−0.01
14	1.98	−0.52	−0.25	−0.12	−0.05	−0.02
15	1.98	−0.37	−0.35	−0.24	−0.12	−0.03
16	1.38	−0.27	−0.24	−0.16	−0.11	−0.05
17	1.98	−0.52	−0.49	−0.34	−0.23	−0.13
18	1.98	−0.95	−0.76	−0.58	−0.58	−0.95
19	2.71	0.23	0.26	0.00	−0.82	−1.16
20	3.50	0.08	0.07	−0.46	−1.18	−1.05
21	2.71	0.14	0.10	−0.02	−0.15	−0.29
22	3.50	0.17	0.13	−0.01	−0.17	−0.31
23	2.71	0.15	0.08	−0.03	−0.09	−0.16
24	3.50	0.05	0.02	−0.05	−0.07	−0.13
25	2.44	−0.05	−0.15	−0.23	−0.09	−0.06
26	2.71	0.11	0.03	−0.05	−0.06	−0.04
27	2.97	0.05	−0.03	−0.05	−0.05	−0.08
28	3.24	0.04	−0.04	−0.07	−0.05	−0.08
29	3.50	0.00	−0.10	−0.18	−0.07	−0.08
30	3.77	−0.02	−0.11	−0.18	−0.13	−0.11
31	2.71	−0.80	−0.95	−1.02	−1.05	−1.16
32	3.50	−0.85	−1.03	−1.06	−1.00	−1.05
33	2.71	−0.83	−0.82	−0.68	−0.51	−0.29
34	3.50	−0.85	−0.85	−0.74	−0.55	−0.31
35	2.71	−0.71	−0.69	−0.53	−0.31	−0.16
36	3.50	−0.73	−0.74	−0.56	−0.28	−0.13
37	2.71	−0.57	−0.59	−0.43	−0.11	−0.04
38	2.97	−0.58	−0.61	−0.45	−0.18	−0.08
39	3.24	−0.56	−0.59	−0.46	−0.19	−0.08
40	3.50	−0.58	−0.60	−0.49	−0.24	−0.08
41	3.77	−0.56	−0.60	−0.52	−0.27	−0.11
42	2.44	0.22	0.26	−0.07	−0.77	−1.01
43	2.97	0.22	0.29	−0.16	−0.94	−1.30
44	3.24	0.15	0.15	−0.30	−1.16	−1.21
45	3.77	−0.99	−1.17	−1.01	−0.96	−1.18
46	3.24	−0.94	−1.07	−1.10	−1.09	−1.21
47	2.97	−0.86	−1.00	−1.05	−1.08	−1.30
Int.		−0.55	−0.36	−0.13	−0.03	0.01

Fig.3. Site plan for houses 02 and 03 with tapping point plan for house 02.

TABLE 3

Pressure coefficients for house 02 — seven 3.2 m spans

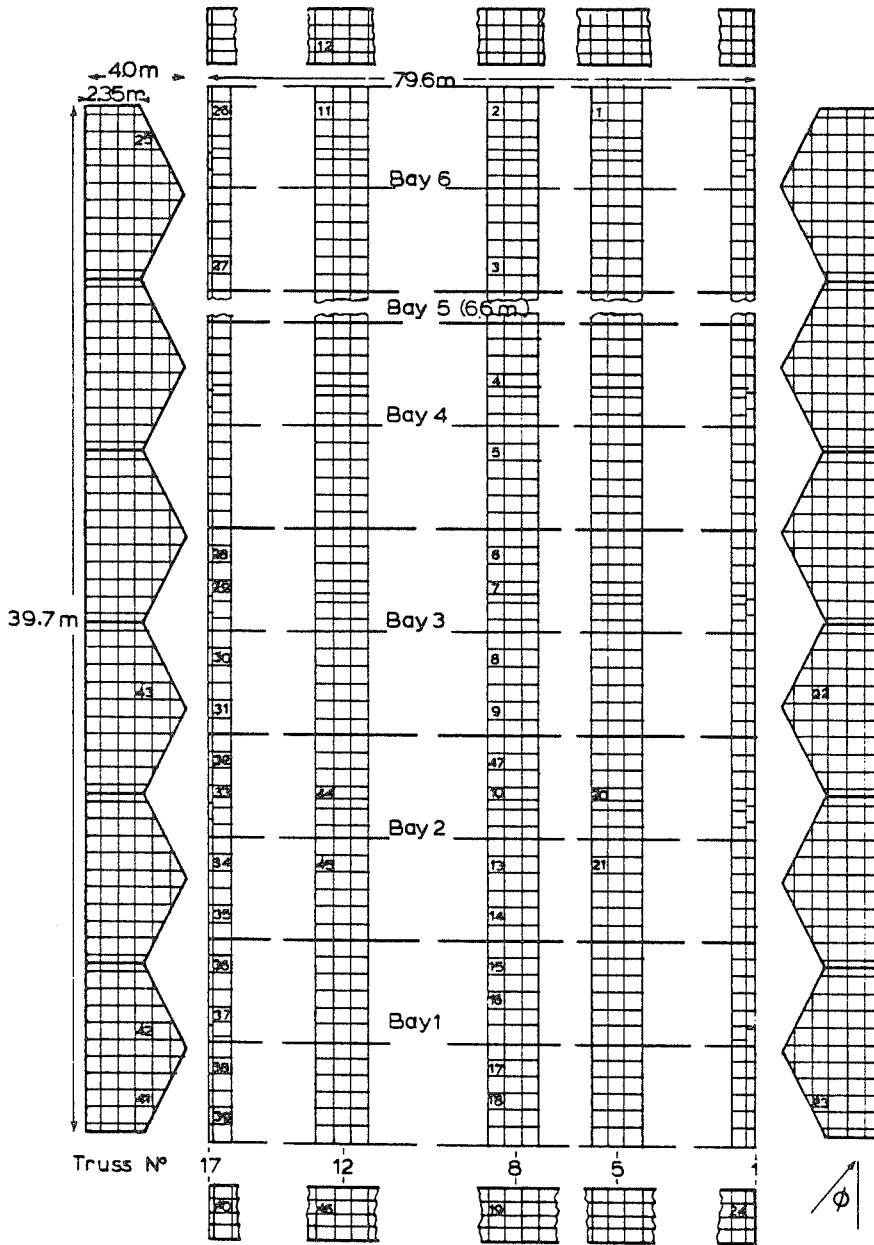| Tapping point		Coefficients relating loads to wind pressure at ridge height ($\alpha = 0.22$)					
No.	Height (m)	Wind angle ϕ (deg)					
		0	22.5	45	67.5	90	112.5
1	2.08	0.65	0.84	0.57	−0.21	−0.75	−0.89
2	2.18	−0.86	−0.34	0.51	0.66	0.50	0.25
3	2.18	−0.81	−0.08	0.58	0.68	0.58	0.39
4	2.18	−0.37	−0.09	0.25	0.49	0.54	0.40
5	2.18	−0.32	−0.03	0.25	0.45	0.55	0.43
6	2.50	−0.74	−0.29	−0.36	−0.58	−0.89	−1.15
7	2.74	−0.52	−0.04	−0.17	−0.67	−1.04	−1.23
8	2.98	−0.30	−0.03	−0.20	−0.81	−1.07	−1.11
9	2.98	−0.78	−1.04	−1.20	−1.22	−1.14	−0.97
10	2.74	−0.75	−1.01	−1.14	−1.16	−1.14	−1.06
11	2.50	−0.73	−0.87	−1.00	−1.18	−1.32	−1.24
12	2.50	−0.46	−0.25	−0.60	−1.04	−1.29	−1.34
13	2.74	−0.38	−0.14	−0.39	−0.90	−1.26	−1.39
14	2.98	−0.35	0.14	−0.34	−0.90	−1.27	−1.42
15	2.98	−0.46	−0.83	−1.17	−1.31	−1.24	−1.06
16	2.74	−0.44	−0.73	−1.10	−1.31	−1.32	−1.18
17	2.50	−0.38	−0.59	−0.99	−1.29	−1.33	−1.19
18	2.50	−0.23	−0.14	−0.60	−1.24	−1.36	−1.38
19	2.74	−0.16	0.07	−0.50	−1.18	−1.38	−1.43
20	2.98	−0.12	0.12	−0.54	−1.13	−1.39	−1.43
21	2.98	−0.35					
22	2.74	−0.31					
23	2.50	−0.26					
24	2.08	0.52	0.33	0.08	−0.05	−0.12	−0.18
25	2.50	−1.30	−1.31	−1.08	−0.39	−0.18	−0.83
26	2.74	−0.62	−0.74	−0.66	−0.32	−0.12	−0.22
27	2.98	−0.37	−0.41	−0.42	−0.37	−0.20	−0.21
28	2.98	−0.80	−0.82	−0.77	−0.57	−0.22	−0.16
29	2.74	−0.96	−0.91	−0.71	−0.41	−0.22	−0.14
30	2.50	−1.06	−0.99	−0.73	−0.39	−0.22	−0.18
31	2.50	−0.96	−0.93	−0.76	−0.48	−0.22	−0.18
32	2.74	−0.65	−0.66	−0.62	−0.49	−0.26	−0.20
33	2.98	−0.50	−0.52	−0.51	−0.41	−0.23	−0.20
34	2.98	−0.50	−0.47	−0.40	−0.31	−0.21	−0.16
35	2.74	−0.44	−0.43	−0.37	−0.30	−0.21	−0.16
36	2.50	−0.42	−0.41	−0.36	−0.29	−0.20	−0.16
37	2.50	−0.39	−0.40	−0.36	−0.29	−0.20	−0.18
38	2.74	−0.28	−0.30	−0.30	−0.23	−0.17	−0.23
39	2.98	−0.20	−0.26	−0.31	−0.27	−0.18	−0.19
40	2.98	−0.42	−0.45	−0.44	−0.32	−0.19	−0.16
41	2.74	−0.42	−0.44	−0.42	−0.29	−0.18	−0.18
42	2.50	−0.36	−0.39	−0.41	−0.33	−0.20	−0.19
43	2.08	−0.32	−0.46	−0.61	−0.88	−0.97	−0.42
44	2.08	0.08	0.04	−0.02	−0.10	−0.12	−0.08
45	2.18	−0.42	−0.52	−0.60	−0.64	−0.50	−0.46
46	2.18	−0.24	−0.38	−0.46	−0.48	−0.36	−0.33
47	2.08	−0.24	−0.35	−0.58	−0.80	−0.65	−0.12
Int. 1		−0.10	−0.19	−0.34	−0.24	−0.15	−0.22
Int. 2 Vents 5—10% open		−0.25				−0.22	

150

Fig. 4. Tapping point plan for house 03.

TABLE 4

Pressure coefficients for house 03 — six 6.6 m spans

Tapping point		Coefficients relating loads to wind pressure at ridge height					
No.	Height (m)	Wind angle φ (deg)					
		−22.5	0	22.5	45	67.5	90
1	2.74	−0.54	−0.55	−0.50	−0.42	−0.31	−0.21
2	2.74	−0.54	−0.56	−0.54	−0.45	−0.32	−0.25
3	2.74	−0.40	−0.43	−0.40	−0.33	−0.26	−0.20
4	3.27	−0.50	−0.52	−0.50	−0.42	−0.33	−0.22
5	3.54	−0.23	−0.22	−0.23	−0.21	−0.19	−0.20
6	2.74	−0.50	−0.52	−0.50	−0.43	−0.32	−0.20
7	3.27	−0.51	−0.53	−0.51	−0.45	−0.33	−0.20
8	3.54	−0.33	−0.34	−0.33	−0.30	−0.23	−0.18
9	2.74	−0.52	−0.56	−0.52	−0.41	−0.26	−0.18
10	3.27	−0.61	−0.66	−0.61	−0.45	−0.29	−0.21
11	2.74	−0.50	−0.55	−0.54	−0.46	−0.36	−0.27
12	1.64	−0.44	−0.44	−0.44	−0.42	−0.32	−0.19
13	3.54	−0.87	−1.01	−0.87	−0.57	−0.30	−0.16
14	2.74	−1.14	−1.22	−1.14	−0.84	−0.46	−0.18
15	2.74	−1.13	−1.26	−1.13	−0.69	−0.39	−0.21
16	3.27	−1.08	−1.19	−1.08	−0.72	−0.42	−0.21
17	3.54	−0.23	−0.18	−0.23	−0.27	−0.23	−0.16
18	2.74	−0.15	−0.03	−0.15	−0.28	−0.26	−0.17
19	1.64	0.35	0.66	0.35	0.12	0.00	−0.10
20	3.27	−0.60	−0.64	−0.60	−0.45	−0.29	−0.20
21	3.54	−0.87	−1.01	−0.87	−0.60	−0.32	−0.13
22	2.47	−0.13	−0.30	−0.44	−0.52	−0.36	−0.24
23	2.47	−0.51	−1.59	−1.20	−0.61	−0.45	−0.38
24	1.64	0.44	0.25	−0.05	−0.17	−0.22	−0.23
25	2.47	−0.30	−0.40	−0.40	−0.25	0.16	0.57
26	2.74	−0.32	−0.55	−0.87	−1.18	−1.71	−1.67
27	2.74	−0.28	−0.18	−0.43	−0.86	−1.27	−1.42
28	2.74	−0.26	−0.50	−0.87	−1.24	−1.67	−1.70
29	3.27	−0.30	−0.55	−0.99	−1.35	−1.56	−1.46
30	3.54	−0.35	0.02	−0.02	−0.54	−1.42	−1.87
31	2.74	−0.40	−0.15	−0.27	−0.68	−1.17	−1.52
32	2.74	−0.29	−0.49	−0.87	−1.11	−1.44	−1.70
33	3.27	−0.33	−0.56	−0.94	−1.24	−1.55	−1.65
34	3.54	−0.59	−0.15	0.08	−0.40	−1.11	−1.48
35	2.74	−0.84	−0.63	−0.04	−0.52	−0.95	−1.36
36	2.74	−0.79	−1.18	−1.27	−0.96	−1.24	−1.42
37	3.27	−0.75	−1.35	−1.29	−1.27	−1.52	−1.53
38	3.54	−0.30	−0.22	−0.08	−0.23	−0.87	−1.56
39	2.74	−0.20	−0.08	0.13	0.13	−0.62	−1.67
40	1.64	−0.05	0.24	0.49	0.41	−0.07	−0.74
41	2.47	−1.22	−1.59	−0.51	0.34	0.70	0.57
42	2.47	−1.12	−1.06	−0.42	0.19	0.61	0.72
43	2.47	−0.44	−0.30	−0.13	0.01	0.35	0.50
44	3.27	−0.60	−0.64	−0.60	−0.46	−0.31	−0.22
45	3.54	−0.87	−1.01	−0.87	−0.47	−0.26	−0.14
46	1.64	0.26	0.46	0.28	0.13	−0.04	−0.14
47	2.74	−0.59	−0.66	−0.59	−0.42	−0.27	−0.19
Int.		−0.40	−0.43	−0.40	−0.33	−0.26	−0.24

Experimental House

N

2.5 m high
deciduous hedge

5 m high
bungalow

10 m high
anemometer

1.5 m high bank

Ground falls away
to south approx
1 in 40 slope

Ø

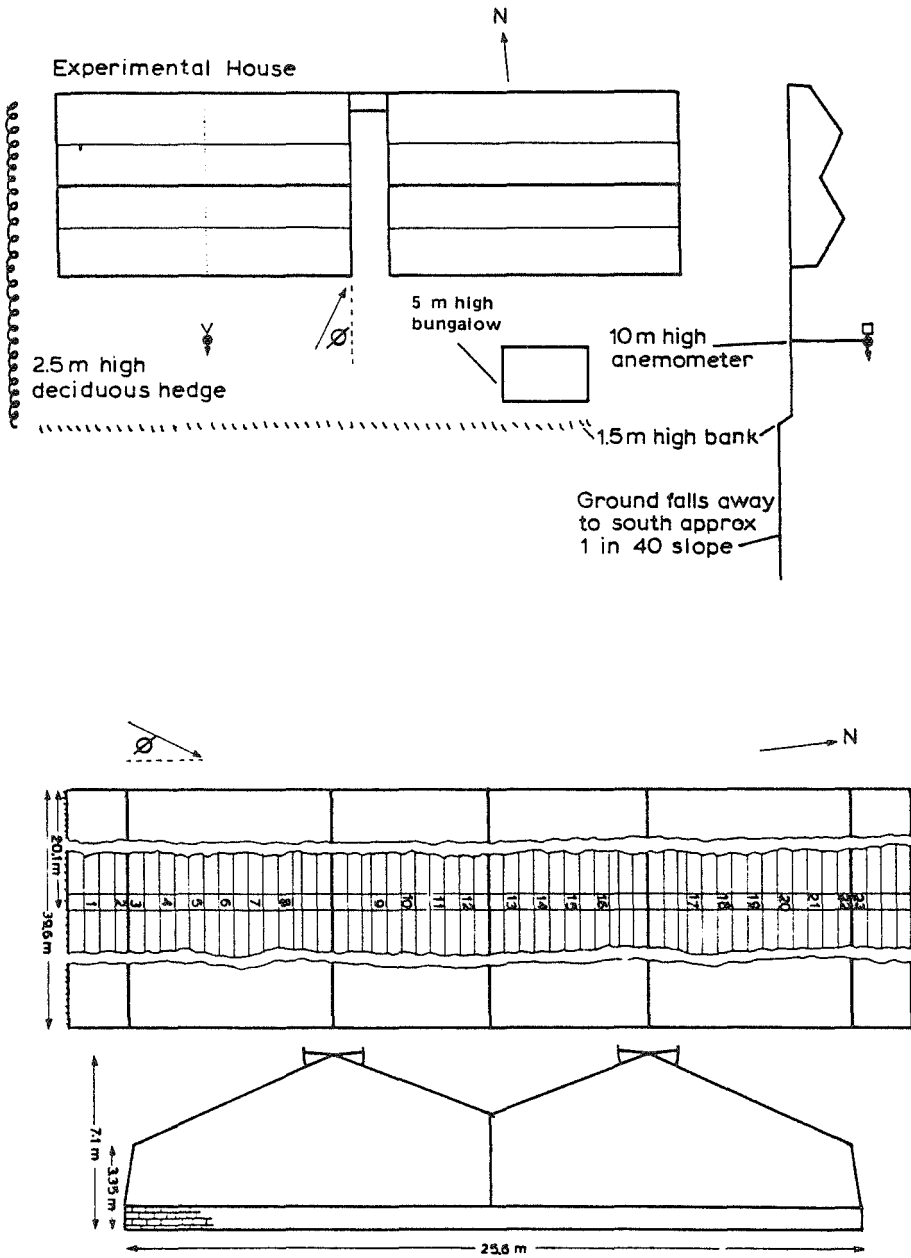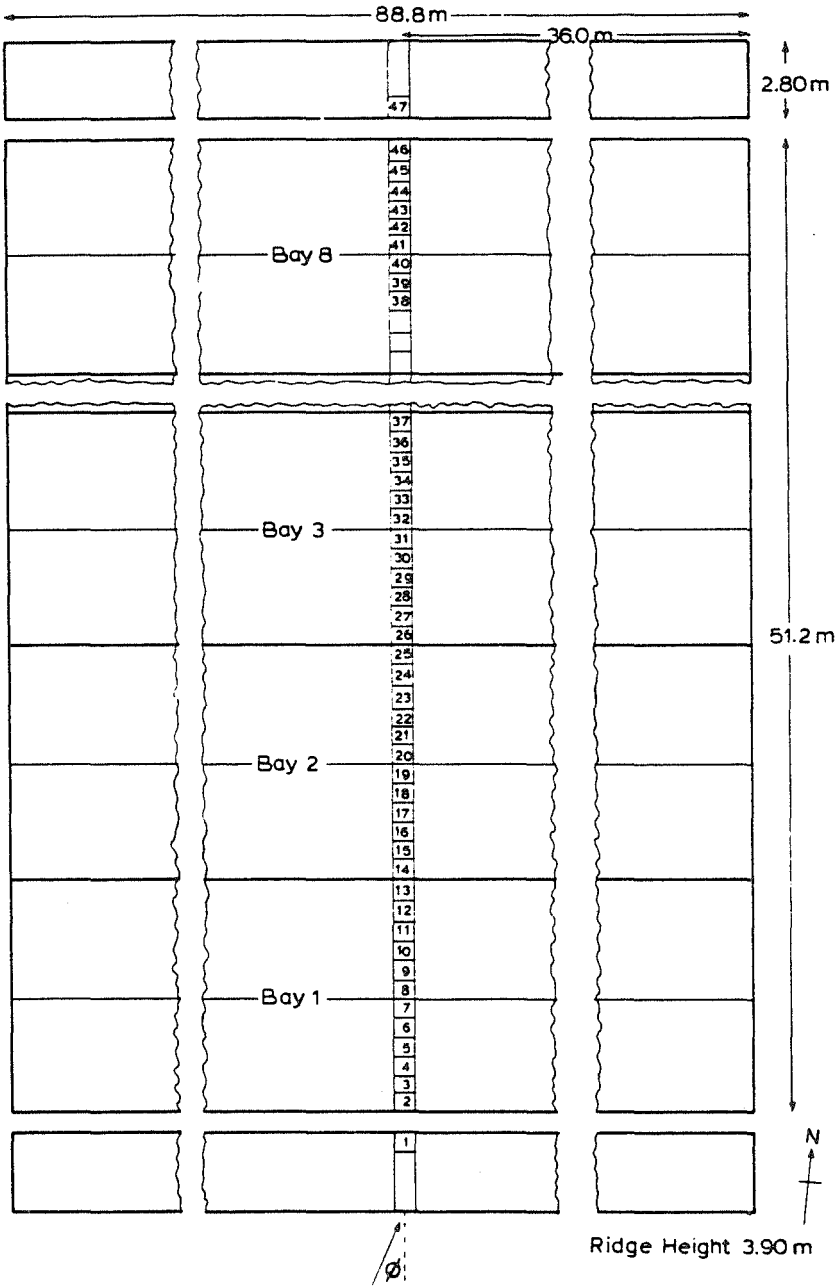N

20.1m

39.6 m

7.1 m

1.35 m

25.6 m

Fig.5. Site and tapping point plan for house 04.

TABLE 5

Pressure coefficients for house 04 — two 12.8 m spans

Tapping point		Coefficients relating loads to wind pressure at ridge height ($\alpha = 0.21$)		
No.	Height (m)	Wind angle ϕ (deg)		
		0	22.5	45
1	1.83	0.58	0.41	0.16
2	3.05	0.67	0.47	0.17
3	3.48	0.25	0.13	0.00
4	4.01	0.39	0.25	0.08
5	4.54	0.38	0.24	0.07
6	5.06	0.25	0.17	0.08
7	5.59	0.25	0.17	0.08
8	6.11	0.22	0.15	0.05
9	6.11	—0.44	—0.35	—0.18
10	5.59	—0.48	—0.43	—0.29
11	5.06	—0.47	—0.46	—0.47
12	4.54	—0.47	—0.41	—0.31
13	4.54	—0.47	—0.43	—0.32
14	5.06	—0.57	—0.43	—0.20
15	5.59	—0.50	—0.33	0.06
16	6.11	—0.48	—0.18	0.10
17	6.11	—0.33	—0.33	—0.31
18	5.59	—0.29	—0.30	—0.30
19	5.06	—0.26	—0.27	—0.30
20	4.54	—0.22	—0.24	—0.26
21	4.01	—0.21	—0.21	—0.19
22	3.48	—0.22	—0.23	—0.26
23	3.05	—0.11	—0.12	—0.13
Int.		—0.11	—0.10	—0.07

Fig.6. Tapping point plan for house 05.

TABLE 6

Pressure coefficients for house 05 — eight 6.4 m spans

Tapping point		Coefficients relating loads to wind pressure at ridge height		
No.	Height (m)	Wind angle ϕ (deg)		
		0	22.5	45
1	2.25	0.32	0.27	0.14
2	2.84	−1.38	−1.39	−1.02
3	3.03	−1.12	−1.10	−0.93
4	3.22	−0.77	−0.73	−0.57
5	3.42	−0.58	−0.58	−0.53
6	3.61	−0.58	−0.58	−0.56
7	3.80	−0.64	−0.65	−0.62
8	3.80	−1.03	−0.98	−0.77
9	3.61	−1.06	−1.00	−0.78
10	3.42	−1.01	−0.94	−0.74
11	3.22	−1.00	−0.95	−0.77
12	3.03	−1.00	−0.94	−0.75
13	2.84	−0.97	−0.93	−0.77
14	2.84	−0.98	−0.95	−0.80
15	3.03	−0.94	−0.89	−0.74
16	3.22	−0.84	−0.79	−0.60
17	3.42	−0.68	−0.66	−0.54
18	3.61	−0.60	−0.57	−0.48
19	3.80	−0.56	−0.56	−0.52
20	3.80	−0.69	−0.66	−0.55
21	3.61	−0.66	−0.63	−0.52
22	3.42	−0.56	−0.52	−0.41
23	3.22	−0.50	−0.47	−0.38
24	3.03	−0.48	−0.46	−0.37
25	2.84	−0.48	−0.47	−0.38
26	2.84	−0.43	−0.41	−0.32
27	3.03	−0.40	−0.39	−0.29
28	3.22	−0.36	−0.34	−0.25
29	3.42	−0.36	−0.34	−0.25
30	3.61	−0.40	−0.38	−0.29
31	3.80	−0.44	−0.42	−0.32
32	3.80	−0.66	−0.64	−0.53
33	3.61	−0.60	−0.58	−0.47
34	3.42	−0.58	−0.55	−0.45
35	3.22	−0.53	−0.51	−0.41
36	3.03	−0.49	−0.48	−0.39
37	2.84	−0.46	−0.44	−0.35
38	3.42	−0.28	−0.26	−0.18
39	3.61	−0.30	−0.30	−0.20
40	3.80	−0.34	−0.32	−0.23
41	3.80	−0.62	−0.59	−0.50
42	3.61	−0.54	−0.50	−0.40
43	3.42	−0.46	−0.43	−0.36
44	3.22	−0.44	−0.41	−0.34
45	3.03	−0.39	−0.37	−0.29
46	2.84	−0.34	−0.32	−0.24
47	2.25	−0.32	−0.29	−0.21
Int.		−0.38	−0.35	−0.26

TABLE 7

Internal pressure coefficients measured in glasshouses of different geometries and glazing systems

Glasshouse description	Height/span	Roof angle (deg)	C_{p_i} transverse	C_{p_i} longitudinal
Single 6.4 m span, length 21.3 m (Cambridge Glasshouse Co.). Overlapped glass (0.61 × 0.61 m) bedded on mastic and clipped at each corner. Continuous ridge vents; doors in centre of both ends.	0.37	26	−0.55	0.01
Seven 3.2 m spans, length 63.0 m (Huisman). Single sheets of glass (1.65 × 0.73 m) between ridge and gutter held in slotted glazing bars. Discrete vents (1 pane in 6); doors in centre of both sides.	0.73	26	−0.10	−0.15
Six 6.6 m spans, length 79.6 m (Cambridge Glasshouse Co.). Overlapped glass (0.61 × 0.61 m) bedded on PVC strip and clipped at each corner. Continuous ridge vents on lee side of each span for transverse wind; doors in centre of both sides.	0.36	26	−0.43	−0.24
Two 12.8 m spans, length 39.6 m (Robinsons of Winchester). Overlapped glass (0.61 × 0.61 m) bedded on PVC strip and clipped at each corner and sides. Continuous ridge vents on both spans; doors in both ends.	0.26	26	−0.11	—
Eight 6.4 m spans, length 88.8 m (Robinsons of Winchester). Overlapped glass (1.65 × 0.73 m) bedded on PVC strip with a metal bar-cap. Fan ventilated glasshouse with 10 fans on each side and continuous ridge ventilators on middle two spans (measurements with fans off), doors in both ends.	0.44	20	−0.38	—
Single 9.15 m span, length 36.6 m (Cambridge Glasshouse Co.). Overlapped glass (0.61 × 0.61 m) bedded on mastic and clipped at each corner. Continuous ridge vents; door in end of lee side.	0.24	26	−0.71	—
Three 6.4 m spans, length 35.0 m (Cambridge Glasshouse Co.). Overlapped glass (0.61 ×0.61 m) bedded on PVC strip and clipped at each corner. Continuous ridge vents on all spans; doors in centre of both ends.	0.39	26	−0.17	—
Three 6.7 m spans, length 40.0 m (Robinsons of Winchester). Overlapped glass (1.65 × 0.73 m) bedded on PVC strip with a metal bar-cap. Continuous ridge vents in each span; doors in centre of both sides.	0.33	20	—	−0.19
Four 9.1 m spans, length 35.0 m (Cambridge Glasshouse Co.). Overlapped glass (0.61 × 0.61 m) bedded on mastic and clipped at each corner. Continuous ridge vents; doors in centre of both ends.	0.26	26	−0.70	—
Nine 15.5 m spans, length 150 m (Wrightrain). Overlapped glass (1.00 × 0.80 m) with plastic bar-cap. Continuous ridge vents in each span; doors in centre of both sides.	0.21	26	−0.62	−0.44
Twelve 3.2 m spans, length 33 m (Westdock). Single sheets of glass (1.65 × 0.73 m) between ridge and gutter held in slotted glazing bars. Discrete vents (1 pane in 6); doors in centre of both ends.	0.72	26	−0.28	—

tions. In all cases, doors and ventilators were closed. For comparison, Table 7 includes internal pressure coefficients for transverse and longitudinal winds for houses 01 to 05.

3.3 Frictional drag

Values are given in Fig.7 of the frictional drag coefficient for houses 01 and 03 under longitudinal winds. The drag coefficient C_f is defined as $C_f = f/q$ where f is the frictional (tangential) force per unit area in the direction of flow and q the wind pressure at ridge height.
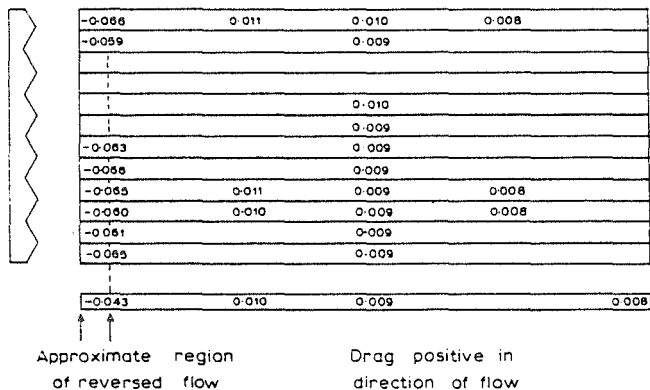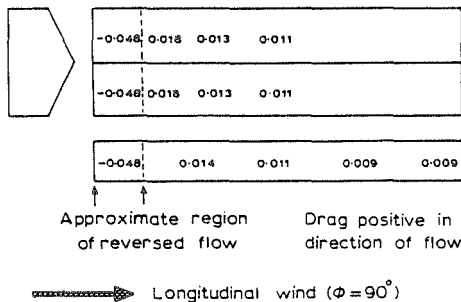

Approximate region of reversed flow   Drag positive in direction of flow

Longitudinal wind ($\Phi = 90°$)

Approximate region of reversed flow   Drag positive in direction of flow

Fig.7. Coefficients of frictional drag for single-span and multi-span houses (01 and 03) under longitudinal wind.

4. Discussion

The pressure coefficients presented in section 3 for five shapes of glasshouse show significantly different loading patterns, and a simple design procedure is not immediately apparent. To illustrate this, a comparison of the results is made which shows the parameters that must be included in a rationalised design procedure.

Results are compared with the pressure coefficients given in CP3 where buildings are categorised by roof angle and height/span parameters.

4.1 *The effect of span width under transverse wind*

Results from three of the multi-span houses (with span widths of 3.2, 6.6 and 12.8 m) show the effect of span width on C_{p_e} for the transverse wind direction. This effect is shown in Fig.8, where the glasshouse section illustrated is an idealised representation and reference must be made to Fig.1 for a comparison of building geometry.
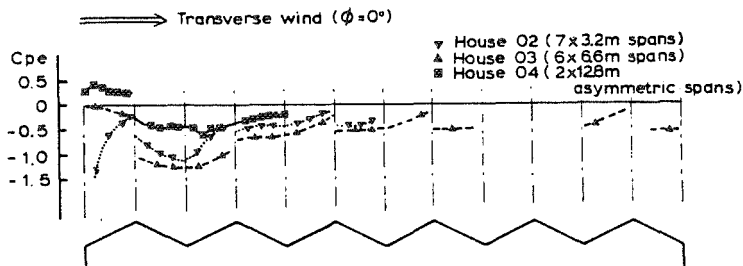
Fig.8. Comparison of C_{pe} for transverse winds on multi-span houses of common roof angle (26°) and variable span.

4.1.1 *Load on windward roof slope*

House 02 (3.2 m spans) has a marked non-uniform loading distribution arising from a region of separated flow extending over most of the roof slope. Such a region of separated flow on the 6.6 and 12.8 m spans is not evident from the pressure pattern which shows the flow to be attached. The marked variation in mean load over the roof slope can be related to height/span ratio (a method adopted in CP3). This is presented in Fig.9 and a comparison is made with CP3 data for single and multi-span buildings.

It is evident from Fig.9 that a single value for load, covering height/span
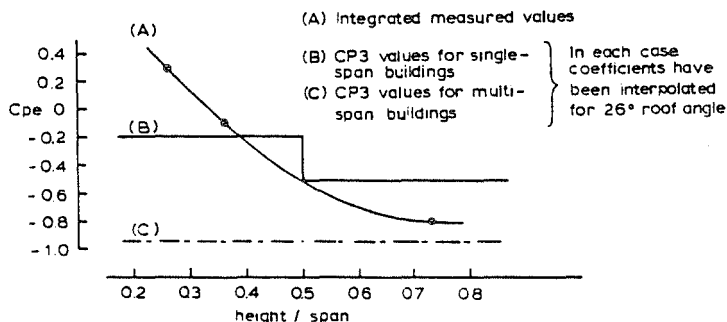
Fig.9. Comparison of integrated values of windward roof C_{pe} related to building height/ span ratio (roof angle 26°).

ratios over the range 0.2—0.8 is not a satisfactory representation. The use of a variable function of height/span is preferable, or alternatively its partitioning into smaller increments.

4.1.2 Load on first leeward roof slope

The distribution of load (Fig.8) is similar for each building, showing pressure decreasing between ridge and valley gutter. The magnitude of mean load is, however, not consistent with the pattern for the windward roof slope, i.e. is not a discernible function of height/span, and the geometric parameters to which it relates are not evident. For glasshouses, the three spans of 3.2, 6.4 and 12.8 m include all popular configurations and the results presented are sufficient for their design; it is, therefore, convenient to express load in terms of span, no generalisation being possible.

4.1.3 Load on second span

Here, again, the distribution of load is similar for each building, with the mean load on the windward roof slope following the pattern on the first leeward roof slope. The mean loads for the three houses begin to converge to a common value on the leeward roof slope of the second span, although the 12.8 m span house is not directly comparable since it is only a two-span structure. The variation in load on the second span can again best be expressed in terms of span for design purposes.

4.1.4 Load on third and subsequent spans

Limited measurements were made on the third, fourth and sixth spans of the 6.6 m span glasshouse and more detailed measurements on the third span of the 3.2 m house. The results show a consistent load distribution for all spans including the leeward roof slope of the last span and mean pressure coefficients can be given, one for all windward roof slopes and another for all leeward roof slopes.

4.2 The effect of roof angle under transverse wind

Only a limited study of the effect of roof angle has been possible.

A comparison is made in Fig.10 of the pressure coefficients for transverse
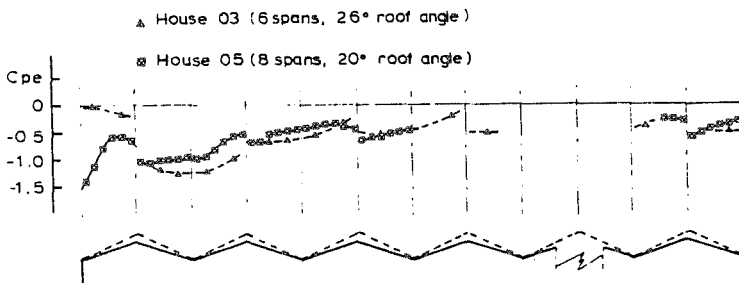
Fig.10. Comparison of C_{pe} for transverse wind on multi-span houses of common span (6.4 m) and variable roof angle.

wind over a six-span 26° roof-angle house (03) and an eight-span 20° roof-angle house (05). These houses are of similar span and exhibit a similar loading pattern over the structure, with the exception of the windward roof slope where the effect of roof pitch is evident. Mean pressure coefficients for the windward roof slope are presented in Table 8 and comparison made with CP3 data.

The values given from CP3 include local coefficients which apply over the upper and lower 20% of the roof slope. Although the marked separation on the 20° roof yields pressure coefficients as low as —1.5, there is no further evidence of other regions where local coefficients should be applied for transverse wind.

TABLE 8

Pressure coefficients for the windward roof slope

Roof angle (deg)	Height/span	External pressure coefficients	
		Full-scale measurements	CP3,Ch.5,Pt.2
20	0.44	—0.84	—1.1
26	0.36	—0.09	—1.0[*]

[*]Interpolated value.

4.3 Comparison of loads on a single-span and on the first span of a multi-span glasshouse under transverse wind

Houses 01 and 03 are of the same design and of identical span section. For the transverse wind direction, a comparison is shown in Fig.11 of pressure coefficients on the single-span house 01 and on the first span of the six-span house 03. The windward wall and roof slope show similar loadings, the small difference may in part be attributed to the different lengths of the two buildings (21.3 m for house 01, 79.6 m for house 03). The load on the leeward roof slope shows a marked effect of the second span, mean pressure coefficients being —0.57 for the single-span and —1.20 for the multi-span. For wind-sensitive structures, such as glasshouses, the design of single- and multi-span structures should therefore be considered separately.

It is again evident from Fig.11 that the concept of regions where local coefficients apply is not supported by full-scale measurements for buildings of 26° roof slope; loads for each surface can be considered as uniformly distributed.

4.4 Roof loads for longitudinal wind direction

The distribution of load on the roof of a single-span and on multi-span houses is shown in Fig.12 for longitudinal wind. The rapid change near the windward end is insufficiently defined for the multi-span houses and the
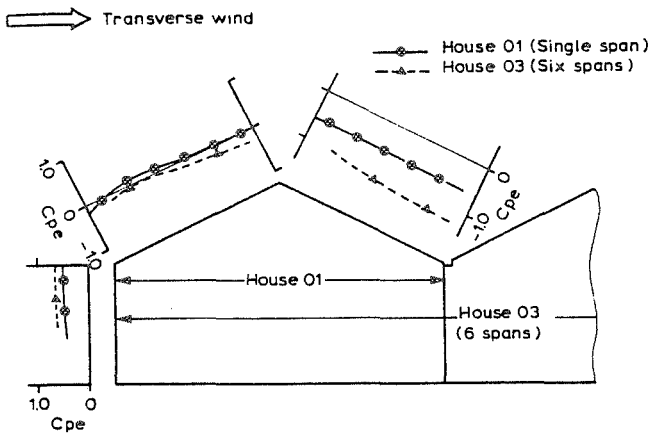
Fig.11. Comparison of C_{pe} for single-span and multi-span houses of identical sectional geometry.
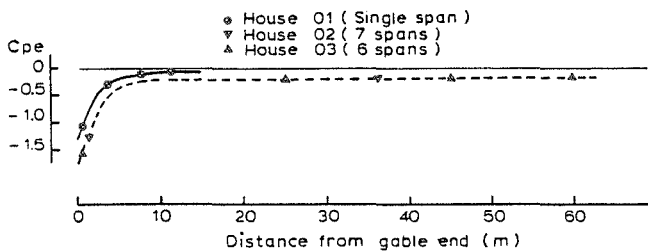

Fig.12. Comparison of C_{pe} for roofs of single-span and multi-span houses under longitudinal wind.

pattern measured on the single-span has been assumed. The difference between load on a single-span and on multi-span houses is small, as is the load on the outer span and inner spans of multi-span houses. A common approach can therefore be adopted in designing all glasshouses for longitudinal wind direction.

4.5 Loads for wind directions other than normal to a major face

Although some roof loads are slightly more severe for wind directions other than normal to a major face of the building, the difference is not significant, and is unlikely to justify consideration in design.

There are a few possible exceptions to this for the side walls where, for example, the maximum suction on the leeward wall can occur at a wind angle of 70° from normal to the windward wall. This applies over a limited region of the wall only, the extent can be estimated from the information in Table 3 (tapping points 43 and 47) and Table 4 (tapping point 12). Other examples can be found, but none is likely to influence structural design.

This simplifies the codification of the results for design purposes, limiting the consideration of wind direction to the major axes of the building.

4.6 Internal pressure coefficients (C_{pi})

The values of internal coefficients given in Table 7 show considerable variation, particularly for transverse winds, where the mean internal pressure in 10 houses can be defined by $C_{pi} = -0.37$ with a standard deviation of 0.22 (referred to the 5 s gust speed at ridge height). Corresponding values for longitudinal wind derived from measurements on five houses are $C_{pi} = -0.18$, with a standard deviation of 0.14.

To take account of the measured variation by applying the more onerous of the extreme values would be an unrealistic design approach, and a more rational procedure is called for.

For the very limited sample in the longitudinal wind case, the internal pressure can be shown to bear a relationship to the length/width ratio of the houses, but no such relationship was found for the transverse case. Very poor agreement was obtained between measured values and those derived from mass conservation calculations based on the external pressure distribution. For those latter calculations, it has been assumed that the cladding, of overlapped glass panes, had provided uniformly distributed permeability and it was concluded that this assumption was invalid. Confirmation of this was obtained from measurements on the six-span 39.7 × 79.6 m glasshouse (03) which showed the mean permeability to be 0.00048 m^2 per m^2 of glasshouse surface. The house had conventional overlapped glazing, and for the measured mean permeability to result only from gaps between panes would require these gaps to be 0.29 mm in extent. However, measurements on many panels, similarly glazed, show the gaps at overlaps to be of the order of 0.05 mm. The house cited had continuous ridge ventilators on one side only of each span and the measured permeability would be attained with a mean ventilator opening of 3.2 mm.

Consideration of the design and construction of modern glasshouses leads to the conclusion that their permeability is concentrated along the ventilator cill/slam rail junctions and around door seals. Modern continuous ridge ventilators are almost always operated by racks which engage with pinions rotated by a continuous torque tube running the length of each ventilator. Deflection of the ventilator cill of a typical design of house will allow an opening of 1 mm to occur midway between the operating racks for each 73 N m^{-2} of negative load in excess of 72 N m^{-2}. Slack in ventilator cill/rack fastenings, backlash between rack and pinion gear teeth and play in torque tube bearers can result in additive ventilator openings totalling 5 mm at design wind speed.

The continuous clamping of the glass at the sides of glazing runs by capping attached to the glazing bars is now near-standard practice, and the likelihood of an increase of permeability arising from deflection of glass under net suction loads is remote. Certainly, for current designs, the permeability afforded by the wind-induced opening of poorly fitting ventilators will dominate

that from all other sources. The mass-production techniques by which ventilators and their operating gear are manufactured and assembled are such as to justify the assumption that such permeability will be uniformly distributed along the ventilator perimeter.

Excellent agreement has been obtained between internal pressures calculated on this basis and those measured in the two houses (01, 03) for which the external pressure distribution was sufficiently detailed for the comparison to be made. For these houses, mass flow directly proportional to permeability (related to seal perimeter) was assumed, and, in view of the known poor seal of the doors, their permeability was taken as twice that of ventilators. Mass flow was taken as proportional to the square root of the pressure difference across the 'seal' and, in the case of ventilators under transverse winds only, an adjustment was made to the external pressure to allow for the effects of the upstand of the ventilators cills. The effect is analogous to that determined for the upstand of glazing bars [12] and results in a 20% reduction or increase, for leeward and inboard windward ventilators respectively, of the external suction.

The adjustments, however, tend to cancel each other out and, in view of the variation in ventilator cill design, the effect has been ignored in the simplified presentation of data in the appendix.

Little guidance on design values of C_{pi} is given by CP3, the most relevant example relates to a dominant opening in a single face and is thus not applicable to pitch-roof glasshouses having a number of openings in the roof. The estimation of C_{pi} by mass conservation calculations, outlined above, is in accord with the fundamental principles detailed in the Wind Loading Handbook [15] which is complementary to CP3.

4.7 Frictional drag

The values given in Fig.7 for the frictional drag coefficient are based on measurements of profile drag of the glazing bar upstand which constitutes the major drag force.

The frictional drag (F) given in section 7.4 of CP3 and which is applicable for the longitudinal wind direction takes the form:

$$F = C_f \cdot q \, (L-4h) \cdot 2h + C_f \cdot q \, (L-4h) \cdot S$$
$$\text{(drag on sidewalls)} \qquad \text{(drag on roof)}$$

where h is the height to the eaves. The coefficient of drag for a glasshouse surface has been derived from measurements and an average value suitable for the above formula is $C_f = 0.01$.

For the transverse wind direction, drag on the roof can be ignored since an extensive part of the roof surface is affected by reverse flow, and the drag of the gable ends can be calculated with $C_f = 0.01$ and

$$F = C_f \cdot q \cdot 2h \, (S-4h)$$

provided the width S is greater than $4h$, otherwise drag can be ignored.

5. Concluding remarks

The work described in this paper is the most detailed full-scale study of the wind loads on glasshouses known to have been undertaken. The results provide reliable and detailed information on the distribution of wind loads and will permit designs to achieve a more effective compromise between the requirements of adequate strength and high light transmission of the structure.

The detailed data have been summarised into a coding format (appendix) for consideration in the context of the general design procedure of CP3.

The validity of the detailed data and coding is limited to the height/span ratios and roof angles of commercial glasshouses.

It had hitherto been considered that internal pressure would be entirely dependent on the effect of the external pressure distribution on the flow of air through the overlaps of the glass cladding. The gaps between panes of glass at overlaps, however, were found to be far too small to account for the measured overall permeability of a large glasshouse.

Consideration of modern glasshouse constructional features leads to the conclusion that ventilators and doors constitute the major sites of permeability and that only these should normally be taken into account in the estimation of internal pressures by mass conservation methods.

CP3 gives a value of frictional coefficient of 0.04 for surfaces with ribs across the wind direction. A value of 0.01 is proposed in this paper, since measurements of the pressure distribution across glazing modules of a full-scale glasshouse indicate this lower value to be more appropriate for the slight ribbing of the surface, constituted by the upstand of the glazing bars.

Acknowledgements

References

1 Glasshouse and glasshouse equipment — England and Wales — Special Enquiry, Stats. 185/73 MAFF Agric. Censuses and Survey Branch, London, 1973.

2 H.C. Shellard, Proc. 1st Int. Conf. on Wind Effects on Buildings and Structures, National Physical Laboratory, London, 1963.

3 CP3, Basic data for the design of buildings, Ch.V, Loading, Pt. 2, Wind loads, British Standards Institution, London, 1972.

4 J.B. Menzies, Wind loads on low-rise structures, BRS News No.13, Building Research Station, Garston. 1970.

5 W.R. Schriever, D.E. Allen and W.A. Dalgliesh, Measurements of snow and wind loads on full-scale buildings for improved design, Tech. Paper 439, National Research Council (of Canada), Division of Building Research, 1975.

6 C. Scruton, Wind effects on structures, Proc. Inst. Mech. Engrs, 185 (1970—71) 301—317.

7 R.P. Hoxey and D.A. Wells, Instrumentation for glasshouse wind load measurements, J. Agric. Engng. Res. 19 (1974) 435—438.

8 R.P. Hoxey and D.A. Wells, Full-scale measurements of wind loads on glasshouses, Proc. Symp. on Full-Scale Fluid Dynamics Measurements, Dept. of Engng., Univ. of Leicester, July 1974, 47—56.

9 Handbook of Meteorological Instruments Pt.1, Instruments for Surface Observations, Meteorological Office, H.M.S.O., London, 1956.

10 R.P. Hoxey, Full-scale wind pressure and load experiments — Wind structure below a height of 10 m, Dept. Note DN/G/678/2301, National Institute of Agricultural Engineering, Silsoe, 1976.

11 J.E. Mayne, A wind pressure transducer, J. Phys. E: Sci. Instrum., 3 (1970) 248—250.

12 R.P. Hoxey, Full-scale wind load and pressure experiments — Effects caused by the glazing bar upstand, Dept. Note DN/G/736/2301, National Institute of Agricultural Engineering, Silsoe, 1976.

13 R.P. Hoxey, An improved method of analysing wind load data, Dept. Note DN/G/825/04024, National Institute of Agricultural Engineering, Silsoe, 1978.

14 K.J. Eaton and J.E. Mayne, The measurement of wind pressures on two-storey houses at Aylesbury, Current Paper CP70/74, Building Research Station, Garston, 1974.

15 C.W. Newberry and K.J. Eaton, Wind Loading Handbook, DoE, H.M.S.O., London, 1974.

Appendix

In deriving loads using the coefficients in this appendix, the design wind speed should be calculated using the S_2 factor appropriate to the *ridge* height of the glasshouse.

TABLE A1

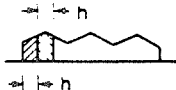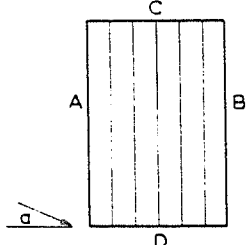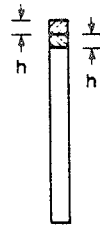Pressure coefficients C_{p_e} for the walls of rectangular glasshouses (single and multi-span structures)

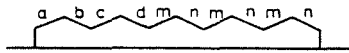| Wind angle α (deg)	C_{p_e} for surface				Local C_{p_e}	
	A	B	C	D	▨	▧
0	+0.6	−0.4	−0.3	−0.3	−1.2	−0.6
					on gable ends C,D	
90	−0.2	−0.2	+0.7	−0.4	−1.0	−0.5
					on side walls, A,B	

TABLE A2

Pressure coefficients C_{p_e} for pitch roofs of rectangular glasshouses

(a) Single-span
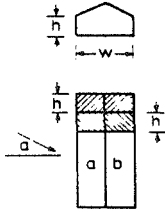
Wind angle α (deg)	Roof angle (deg)	C_{p_e} a	b	Local C_{p_e} ▨	▧
0	26	see Fig.A1	−0.6	−1.0	−0.8 on roof slope b only
	20	see Fig.A1	−0.6	−1.0	−0.8 on roof slope b only
90	20—26	−0.2	−0.2	−1.2	−0.5

(b) Multi-span

Wind angle α (deg)	Roof angle (deg)	h/w	C_{p_e} First spans a*	b	Second span c	d	Other spans m	n	Local C_{p_e}** ▱	▨
0	26	0.26	+0.3	−0.5	−0.5					
		0.36	−0.1	−1.2	−1.1	−0.6	−0.4	−0.5	—	—
		0.73	−0.8	−1.0	−0.7					
0	20	0.44	−0.85	−1.0	−0.8					
90	20—26	all	−0.2	−0.2	−0.2	−0.2	−0.2	−0.2	−1.4	−0.6

*As for single-span, i.e. pressure coefficients from Fig.A1.
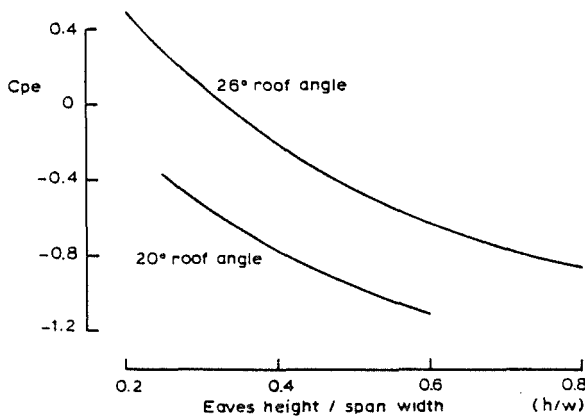**As designated for single-span and to be applied to all spans.


Fig.A1. Pressure coefficients for first roof slope.

Internal pressure coefficients for rectangular glasshouses

For each wind direction being considered, a design internal pressure should be derived such that air flow into the glasshouse equals that extracted, consideration being given to the size and position of openings relative to the external pressure distribution. The openings in a glasshouse may normally be considered to be limited to the perimeter of the seals of ventilators and doors.

Mass flow should be taken as proportional to the area of the leakage paths and to the square root of the pressure difference across them.

TABLE A3

Frictional drag
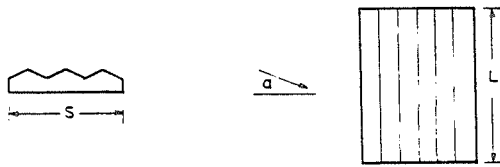
Wind angle α (deg)	Frictional drag (F)
0	$F = C_f \cdot 2h \, (S-4h) \cdot q$ provided $S > 4h$, otherwise frictional drag can be ignored
90	$F = C_f \cdot 2h \, (L-4h) \cdot q \; + \; C_f \cdot S \, (L-4h) \cdot q$ provided $L > 4h$

The coefficient of frictional drag for the above is $C_f = 0.01$ and q is the dynamic pressure of the wind derived from the design wind speed.